

# The Effectiveness of Surface Coatings on Preventing Interfacial Reaction During Ultrasonic Welding of Aluminum to Magnesium

ALEXANDRIA PANTELI, JOSEPH D. ROBSON, YING-CHUN CHEN,  
and PHILIP B. PRANGNELL

High power ultrasonic spot welding (USW) is a solid-state joining process that is advantageous for welding difficult dissimilar material couples, like magnesium to aluminum. USW is also a useful technique for testing methods of controlling interfacial reaction in welding as the interface is not greatly displaced by the process. However, the high strain rate deformation in USW has been found to accelerate intermetallic compound (IMC) formation and a thick  $\text{Al}_{12}\text{Mg}_{17}$  and  $\text{Al}_3\text{Mg}_2$  reaction layer forms after relatively short welding times. In this work, we have investigated the potential of two approaches for reducing the IMC reaction rate in dissimilar Al-Mg ultrasonic welds, both involving coatings on the Mg sheet surface to (i) separate the joint line from the weld interface, using a 100- $\mu\text{m}$ -thick Al cold spray coating, and (ii) provide a diffusion barrier layer, using a thin manganese physical vapor deposition (PVD) coating. Both methods were found to reduce the level of reaction and increase the failure energy of the welds, but their effectiveness was limited due to issues with coating attachment and survivability during the welding cycle. The effect of the coatings on the joint's interface microstructure, and the fracture behavior have been investigated in detail. Kinetic modeling has been used to show that the benefit of the cold spray coating can be attributed to the reaction rate reverting to that expected under static conditions. This reduces the IMC growth rate by over 50 pct because at the weld line, the high strain rate dynamic deformation in USW normally enhances diffusion through the IMC layer. In comparison, the thin PVD barrier coating was found to rapidly break up early in USW and become dispersed throughout the deformation layer reducing its effectiveness.

DOI: 10.1007/s11661-013-1928-z

© The Author(s) 2013. This article is published with open access at Springerlink.com

## I. INTRODUCTION

IN the near future, automotive design will be based on a multi-material approach, allowing more efficient use to be made of the best attributes of different classes of materials.<sup>[1–3]</sup> This has resulted in heightened interest in welding dissimilar combinations of light metals, such as aluminum and magnesium. Unfortunately, fusion welding processes are very difficult to apply to dissimilar aluminum and magnesium alloy joints because of the rapid formation of intermetallic compounds (IMC) which occurs in the welds.<sup>[4]</sup> As a result, solid-state methods, like friction stir welding (FSW), are attracting increasing interest<sup>[5–9]</sup> as are other solutions such as self-piercing rivets (SPR), clinching, and adhesive bonding.<sup>[10,11]</sup> However, SPR or clinching and bonding have additional consumable and surface treatment costs, and require sufficient formability of the material.

Ultrasonic spot welding (USW) is an alternative solid-state welding technique that has the potential for joining reactive dissimilar metals like aluminum to magnesium. Although USW has been successfully used since the 1950s to join thin sheets of various dissimilar material combinations,<sup>[12,13]</sup> higher power welding systems have only been applied to thicker (1 to 2 mm) automotive gages relatively recently.<sup>[14,15]</sup> In lower power USW, bonding occurs at moderate temperatures [ $<573$  K (300 °C)] and is dominated by contact mechanics, with deformation localized to the weld faying surfaces.<sup>[16,17]</sup> Weld formation initially involves ultrasonic vibration breaking down the surface oxide layer between contacting asperities, resulting in local adhesion and the formation of microwelds, which expand and spread across the weld interface.<sup>[12,16,17]</sup> In contrast, when welding a thicker (~1 mm) gage automotive sheet, because of the higher energy input required, peak temperatures at the interface can reach above 400 °C.<sup>[15,18,19]</sup>

In the Al-Mg joints, the growth kinetics of the IMC phases formed are unusually rapid<sup>[19–21]</sup> and welding is also made more challenging by the presence of low melting point eutectic reactions.<sup>[9,22,23]</sup> In prior research,<sup>[19]</sup> it has been shown that with USW Al-Mg welds can be made that have lap shear strengths equivalent to those found in similar Mg-Mg welds in short welding times of  $<0.5$  seconds. However, the dissimilar welds failed with half the fracture energy and at the interface rather than by nugget

---

ALEXANDRIA PANTELI, Scientist, formerly with the School of Materials, University of Manchester, Manchester, U.K., is now with the AMEC UK Ltd, Warrington, U.K. JOSEPH D. ROBSON, Reader, YING-CHUN CHEN, Research Assistant, and PHILIP B. PRANGNELL, Professor, are with the School of Materials, University of Manchester. Contact e-mail: philip.prangnell@manchester.ac.uk

Manuscript submitted March 27, 2013.

Article published online August 20, 2013

pullout. This poor fracture behavior was related to the rapid development of an IMC reaction layer at the joint interface, which reached  $5\ \mu\text{m}$  thick in only 0.4 seconds. Similar to the behavior seen in research on Al-Mg diffusion couples,<sup>[20,24]</sup> the IMC layer was found to be composed of two phases,  $\gamma\text{-Al}_{12}\text{Mg}_{17}$  and  $\beta\text{-Al}_3\text{Mg}_2$ , which formed as sub-layers on the magnesium and aluminum sides of the welds, respectively.<sup>[19]</sup> In USW, this unusually large IMC layer thickness has been shown to arise not only due to the greater interface temperatures reached, when using sufficient power to weld 1-mm gage sheets, but also because the growth rate was found to be over double that seen under static conditions.<sup>[19]</sup> This accelerated reaction rate was attributed to enhanced diffusion caused in the initiation stage by a high deformation-induced vacancy concentration, generated by the high strain rate in USW,<sup>[18,19,25]</sup> and subsequently by microcracking in the brittle reaction layer as it developed.<sup>[19,26]</sup>

The control of intermetallic formation in Al-Mg bimetallic welding is an important issue that so far has prevented the adoption in service of any safety-critical welded joints between these two materials. In the literature, only a limited number of attempts to control the IMC reaction between aluminum and magnesium in welds have been reported to date, through using interlayers of various materials inserted in the joint interface.<sup>[27,28]</sup> The objectives of this work were to introduce a material between the weld members which forms less detrimental IMCs or that reduces the rate of reaction, by either creating a barrier to diffusion or through introducing a slower diffusing species. Some success has been noted by the use of a zinc interlayer in diffusion bonding aluminum to magnesium, which was found to produce a slower-growing  $\text{MgZn}_2$  Laves-type phase at the interface.<sup>[27]</sup> A cerium foil interlayer has also been used in laser-TIG hybrid welds with a slight increase in weld strength reported.<sup>[28]</sup>

In the work reported here, we have investigated the potential of two approaches for reducing the IMC reaction rate in the Al-Mg welds, both involving coatings on the magnesium sheet surface, with the aim of (i) separating the joint line from the weld interface and (ii) providing a diffusion barrier layer. To achieve the former objective, a thick  $\sim 100\ \mu\text{m}$  aluminum coating was produced on the magnesium sheet using the cold spray method, to create an aluminum surface layer that could then be welded to the aluminum alloy sheet. For the second approach, a thinner  $1\text{-}\mu\text{m}$ -thick manganese (Mn) coating was applied by physical vapor deposition (PVD). Manganese was selected for a barrier material as it has a low diffusivity in aluminum and manganese does not form any IMCs with magnesium.<sup>[29]</sup> The joint's interface structure and in particular the IMC reaction rate, as well as the failure behavior, have subsequently been compared to that of Al-Mg joints produced without a coating interlayer and the results are discussed with the aid of kinetic modeling. Finally, it should be noted that USW is a useful joining technique for testing methods of controlling solid-state interfacial reaction, as the interface is not greatly displaced during welding, and the results of this study are more generally applicable to IMC control in other welding processes where the reaction behavior is more difficult to interpret (*e.g.*, FSW).

## II. EXPERIMENTAL

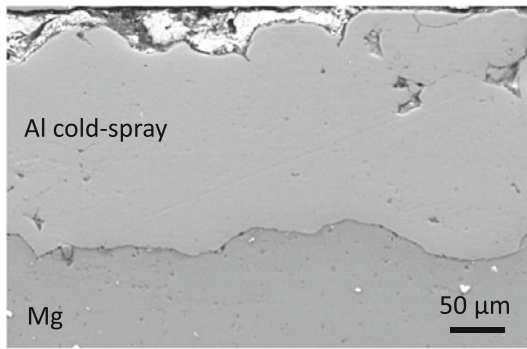
The welds investigated were produced between an aluminum AA6111 and magnesium AZ31 alloy, using 1-mm-thick sheets—in T4 and H24 tempers, respectively. The magnesium sheet was prepared by grinding off its thicker oxide using 320 grit SiC paper, whereas the aluminum sheet was welded in the as-rolled condition. Both materials were thoroughly degreased with ethanol prior to welding. The two coatings discussed above were produced on the magnesium sheet after surface cleaning. The  $100\text{-}\mu\text{m}$ -thick cold spray coating was produced by the Beijing Institute of Aeronautical Materials using commercial purity aluminum powder. This coating technique was selected as it is a low temperature process<sup>[30]</sup> and does not result in an IMC layer being present prior to welding. The thin  $1\ \mu\text{m}$  manganese coating was produced by the Cranfield University surface engineering group using PVD, involving pulsed-DC sputtering with a manganese target. Prior to coating, sputter-ion cleaning was employed to promote the coating adhesion.

USW was carried out with a Sonobond dual-head welder operating at a frequency of 20.5 kHz and a nominal power of 2.5 kW. The materials were welded between two  $9 \times 6\ \text{mm}^2$  sonotrode tips, which had nine parallel teeth orientated perpendicular to the direction of vibration (Reference 15 for full details). Welding was performed with a constant power setting for increasing welding times, using a clamping force of 1.9 kN. Welds were made at the center of a 25-mm overlap on  $100 \times 25\ \text{mm}^2$  coupons with light clamping. The weld temperatures were measured as close as possible to the joint line at the weld center, which is the hottest location in the weld,<sup>[15,18,31]</sup> using sacrificial 0.5-mm K-type thermocouples. Measurements were repeated several times and only averaged over results that gave heating and cooling curves with a consistent profile. Tensile lap shear testing was carried out on the welded samples using a cross-head speed of  $0.5\ \text{mm min}^{-1}$ , with both the peak load and fracture energy (area under the load–displacement curve) measured. Metallographic samples were prepared from the weld cross sections using standard procedures. Imaging was carried out by conventional optical microscopy and with an FEI Sirion, FEG SEM. The average IMC reaction layer thickness was measured at the center of the welds by image analysis on SEM back scattered images, using the area of the IMC layer divided by the interface length, over a  $500\text{-}\mu\text{m}$ -long section of interface.

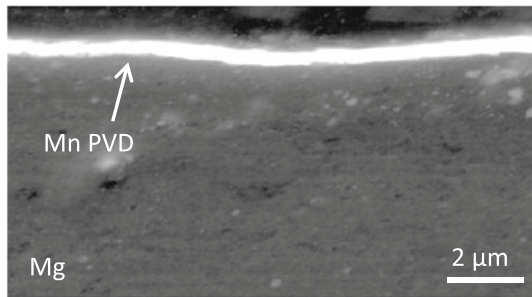
## III. RESULTS

### A. Coatings

Cross sections through the two coatings are shown in Figure 1. The cold spray coating had an average thickness of  $\sim 100\ \mu\text{m}$  and generated a relatively rough surface compared to that of the original magnesium sheet and contained some porosity, but no evidence could be found of an IMC layer between the coating and the magnesium substrate prior to welding (Figure 1(a)).  $R_a$  roughness values (arithmetic average of absolute



(a)



(b)

Fig. 1—SEM images of cross sections through the coatings investigated: (a) the 100- $\mu\text{m}$ -thick aluminum cold spray coating and (b) the thinner 1- $\mu\text{m}$ -thick manganese PVD barrier coating, both applied to the AZ31 magnesium sheet.

amplitude), measured for the surfaces using a  $\mu$ -scan SC200 laser profiler, were found to be 13.7  $\mu\text{m}$  for the cold spray-coated surface compared to 2.7  $\mu\text{m}$  for the original magnesium sheet surface. The thinner Mn-PVD coating is shown in Figure 1(b) and was measured to have an average thickness of 0.92  $\mu\text{m}$ . It provided a high level of coverage, with thinning only apparent in areas where deeper local scratches were present that arose during sample preparation. The PVD coating had little effect on the surface roughness, which was similar to that of the uncoated magnesium sheet ( $R_a = 3.1 \mu\text{m}$ ).

### B. Weld Temperatures

Because heat generation in USW can be affected by the surface contact conditions (e.g., surface roughness, hardness, friction, etc.<sup>[12,17]</sup>), peak temperatures at the weld interfaces were measured when welding with the coated and uncoated magnesium sheets, as a function of welding time, using sacrificial thermocouples, and the results are shown in Figure 2. The data for the manganese-coated welds were more limited, owing to a shortage of material, but overall the results indicated a very similar temperature rise with welding energy/time for all the material combinations. For longer welding durations, the measured interface temperatures were virtually identical and only a small difference could be seen at short times, which suggests that the early rate of heat generation in the welds produced with pre-coated magnesium sheets may have been slightly lower. Hence, for longer welding times, differences in the interface

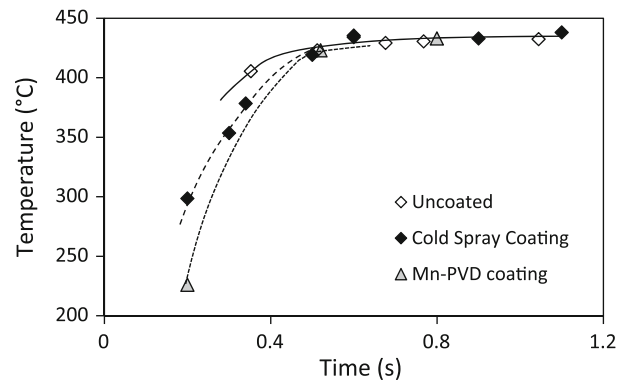


Fig. 2—Maximum interface temperatures recorded by thermocouple measurements, as a function of welding time, for Al-Mg welds produced with uncoated and pre-coated Mg sheet.

reaction behavior, noted below could be directly attributed to the properties of the coatings used, rather than from any indirect influence of the weld temperatures.

### C. Mechanical Performance

The results of tensile lap shear tests performed on the welded samples are shown in Figure 3 for increasing welding times. For short welding times, the maximum failure loads measured with the cold spray-coated samples were almost identical to those achieved for the uncoated sheets (Figure 3(a)). Both sets of data also reached a similar maximum strength level of  $\sim 2 \text{ kN}$ , but for longer welding times, the strength of the uncoated material began to decrease considerably earlier, allowing higher weld energies to be used with the coated magnesium sheet without any loss of shear strength properties. For example, in Figure 3(a) it can be noted that in the uncoated Mg welds the shear strength decayed after a dwell time of 0.4 seconds, whereas the data for the cold spray-coated samples exhibited a plateau that maintained a near-maximum strength level of 2.1 kN until 0.80 seconds, whereafter it decreased at a similar rate. In contrast to the improved performance seen for welds produced with the cold spray-coated magnesium sheet, the failure loads for the manganese-coated samples showed little difference to that of the uncoated samples, across the range of welding times investigated (Figure 3(a)).

Useful information can also be obtained from lap shear test data by considering the failure energy, which is determined by integration of the load–displacement curve. This parameter is more sensitive to changes in the failure behavior than the maximum load.<sup>[15]</sup> An example, comparing two load–displacement curves obtained from welds produced with uncoated and cold spray-coated magnesium sheets for a 0.8 second welding time, is shown in Figure 4 to illustrate the large difference in failure energy (area under the curves) that resulted from using the cold spray-coated magnesium material when using longer welding times, despite the more similar fracture strengths. As can be seen from Figure 3(b), the failure energies for the welds where the magnesium had been cold spray coated showed a



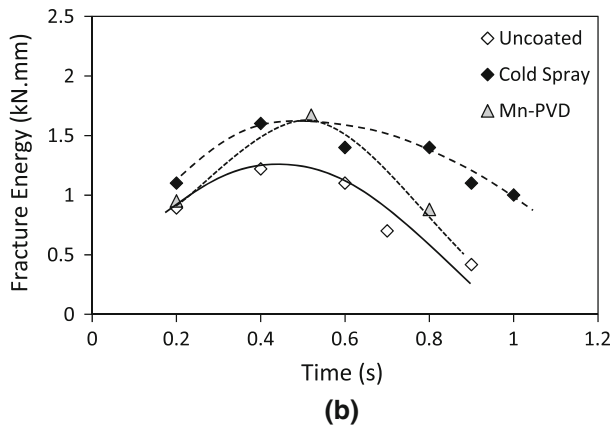
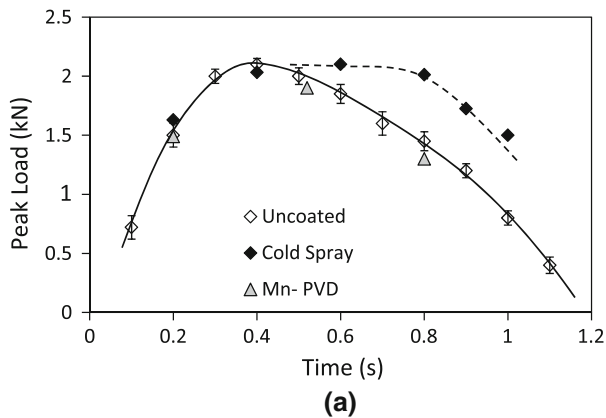


Fig. 3—Lap shear test results, as a function of welding time, showing (a) the peak failure load and (b) the fracture energy of welds produced with cold spray and PVD Mn coatings, compared to results from welds without pre-coating the magnesium.

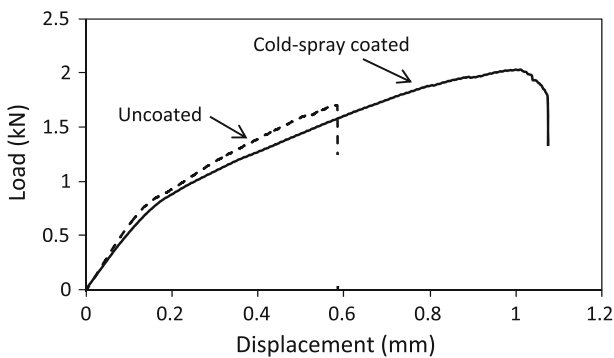


Fig. 4—Comparison between the lap shear test load–displacement curves recorded for a cold spray-coated and -uncoated magnesium sheet, joined to aluminum using USW, with a duration of 0.80 s.

considerable improvement relative to those produced with uncoated sheet. For the optimum welding time of 0.4 seconds, the welds with the uncoated material had a fracture energy of 1.2 kN mm and with the cold spray-coated material this increased to 1.6 kN mm. In addition, the data for the cold spray samples decayed more slowly when a greater than optimum weld energy was applied, resulting in their fracture energy becoming more than double that of the uncoated samples by a welding time of 0.80 seconds. In comparison, the failure energy

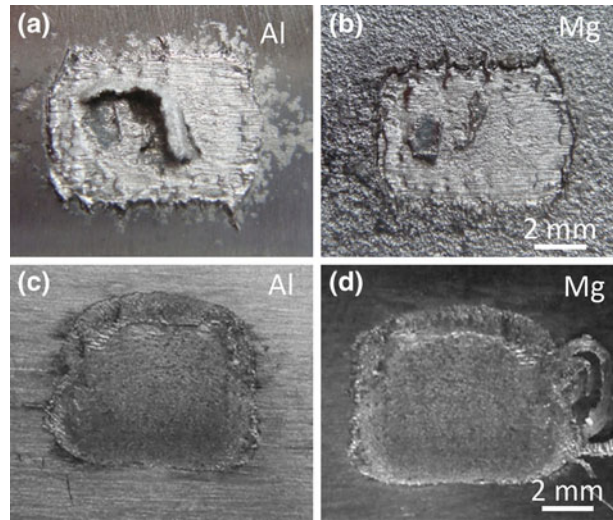


Fig. 5—Examples fracture surfaces from the pre-coated Al-Mg welds for: (a) the aluminum surface that was welded to (b) the cold spray-coated magnesium sheet and (c) the aluminum surface that was welded to the (d) Mn-PVD-coated Mg sheet, both for a welding time of 0.8 s.

of the joints made with manganese-coated magnesium sheet was not as significantly improved. There was still a benefit at shorter welding times (*e.g.*, 0.5 seconds), but the difference was less pronounced at longer welding times (Figure 3(b)).

It has been shown previously<sup>[19]</sup> that failure in lap shear tests of high power USWs, produced under identical conditions, between the same uncoated aluminum and magnesium alloys (*i.e.*, AA6111 and AZ31), always occurs by interfacial fracture, owing to the rapid development of an interfacial IMC reaction layer. Despite having notably higher fracture energies, the pre-coated samples did not exhibit the hoped for step change in the fracture energy that would be associated with a transition from interface fracture to nugget pullout mode and this was reflected in observations of the fracture surfaces, none of which showed a pullout behavior, examples of which are provided in Figure 5. Although a pullout failure was not observed for either type of weld, it can be noted (Figures 5(a) and (b)) that in the case of the thicker cold spray coating, fracture involved partially peeling the aluminum coating off its magnesium substrate. With the much thinner manganese coating (Figures 5(c) and (d)), traces of manganese were also found on both weld member surfaces after fracture by EDS analysis.

#### D. Interfacial Reaction Behavior

The effect of the two coatings on the interfacial reaction behavior in the dissimilar metal welds was studied by SEM on cross sections through their center, examples of which are shown in Figures 6 and 7. The average thickness of the interface reaction layer found in each case at the weld center was also measured and has been plotted against welding time in Figure 8.

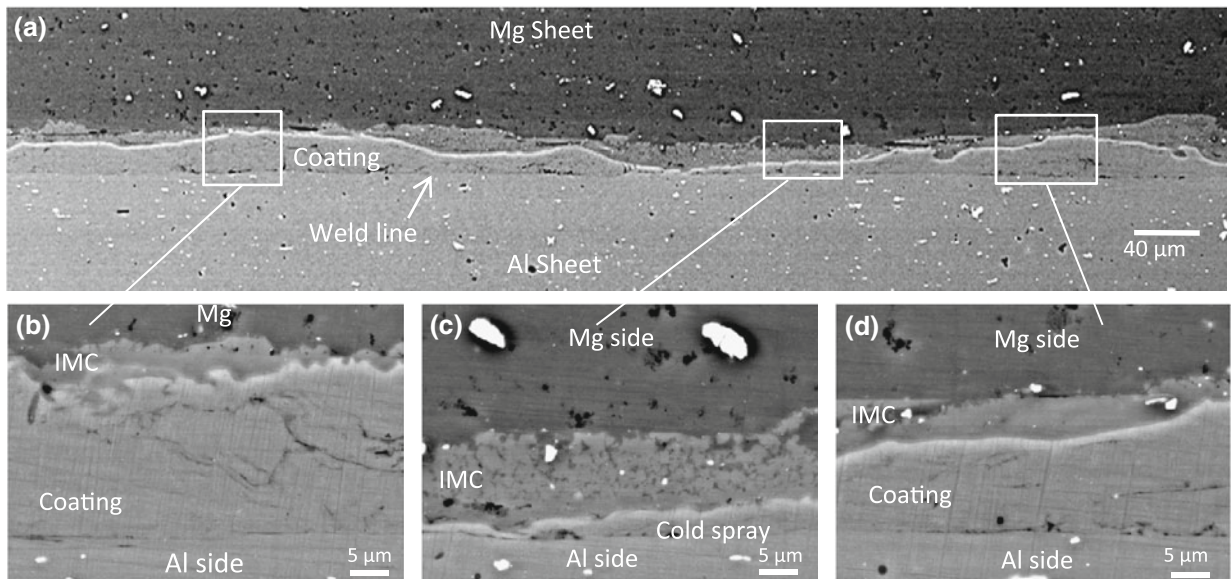


Fig. 6—SEM images showing the IMC reaction layer formed at the interface between the Al cold spray coating and Mg substrate after USW with a welding duration of 0.5 s: (a) overview and (b) through (d) selected areas at higher magnification.

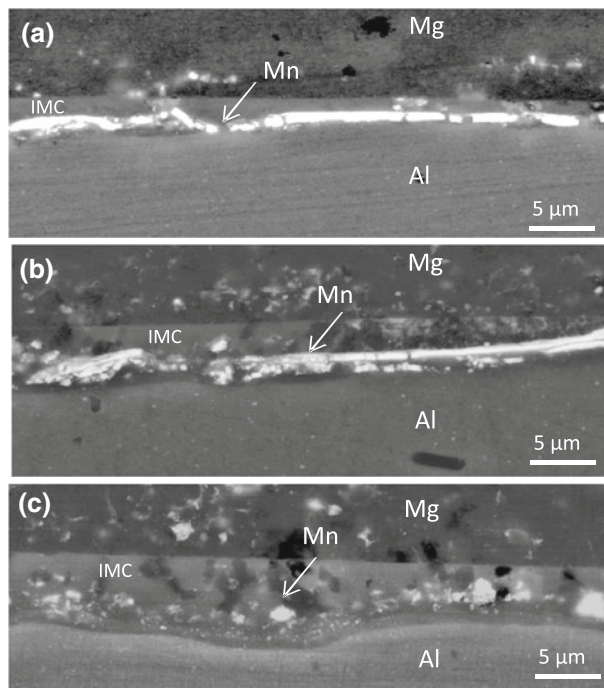


Fig. 7—SEM images showing the breakup of the Mn barrier coating and growth of the IMC reaction layer with increasing welding times of (a) 0.3, (b) 0.7, and (c) 1.1 s.

In the welds produced with the cold spray-coated magnesium sheet, because the weld was formed between two aluminum surfaces, no IMC reaction was expected at the joint line. However, the bimetallic interface between the coating and substrate was still in close proximity to the hottest part of the weld, being displaced from the joint line by only 100  $\mu\text{m}$ . In the welds produced with pre-coated magnesium sheets, the IMC reaction was found to proceed in a similar manner to

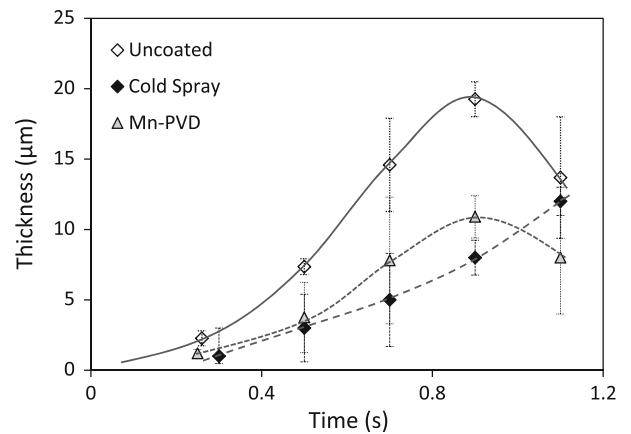


Fig. 8—The average thickness of the Al-Mg interface reaction layer plotted against weld time, for welds produced with cold spray and Mn-PVD coatings, compared to the behavior seen in welds formed with uncoated Mg sheet.

that previously reported between uncoated sheets,<sup>[19]</sup> but as expected it took place at the aluminum coating–magnesium substrate interface rather than at the weld line (Figure 6). However, as can be noted from Figure 8, the overall reaction rate was substantially reduced. For example, at a welding time of 0.7 seconds, the IMC layer in the cold spray-coated joint was on average 5  $\mu\text{m}$  thick, compared to nearly 15  $\mu\text{m}$  in the uncoated sample. In addition, in the case of the pre-coated samples, early formed reaction islands did not fully coalesce until longer weld times of greater than 0.50 seconds, as opposed to 0.25 seconds with uncoated sheet (References 19 and 32). There were also still large variations in the IMC layer thickness for welding times up to 0.90 seconds (Figure 6), whereas when no coating was used, the layer became uniform in thickness by  $\sim$ 0.5 seconds. While there was a lot more variation in



the IMC thickness in the cold spray samples, owing to variability in the coating thickness, the mean layer width was between a third and a half that for the uncoated samples at any given weld time up to 1.10 seconds (Figure 8). For welding times greater than 0.9 seconds, partial melting of the IMC layer in the uncoated samples progressively reduced the layer thickness (this behavior has been previously described in Reference 19), causing the curves to eventually converge (Figure 8). As the IMC layer in the cold spray pre-coated welds was not observed to melt, this suggests that the peak temperature reached at the interface between the coating and the magnesium substrate was slightly lower than at the joint interface.

The lap shear test results above indicated that the manganese coating had a more limited effect on the joint properties than the cold spray coating, although a modest improvement in the failure energy was observed at intermediate welding times (Figure 3). The main reason why the manganese diffusion barrier coating was not as successful can be seen in Figure 7, where the joint interface is shown as a function of welding time. For the shortest welding time (0.3 seconds, Figure 7(a)), it was already apparent that the coating had become damaged by the deformation occurring at the contacting sheet surfaces during the USW welding process<sup>[12,15,16]</sup> and had fractured into smaller segments, some of which have been displaced leaving the surface of the magnesium sheet exposed. The damage to the coating was, however, not very uniform and areas could be seen that were still protected. The damage to the coating became worse with increasing welding time, which became progressively more broken up and dispersed. After welding times in excess of one second (Figure 7(c)), little effective coverage of the coating was retained and largely only particulate debris was observed, which became dispersed within the deformation zone near the joint line and incorporated into the IMC reaction layer.

Despite the failure of the manganese barrier coating, when the reaction layer thickness was averaged over the interface area, the reaction rate was still found to be lower for welds produced with the Mn-PVD coating than without. Overall, the average IMC layer thickness for the coated samples was approximately half that of the uncoated over the range of weld times studied. At a weld time of 0.9 seconds, a maximum IMC layer thickness was observed in welds produced with both uncoated and coated magnesium sheets and at this point, the layer thickness was 19  $\mu\text{m}$  in the uncoated weld and 10  $\mu\text{m}$  in the coated. For longer welding times, the reaction layer in both cases was found to reduce in thickness, suggesting that eutectic melting of the IMC layer<sup>[19]</sup> initiated in both cases at similar welding energies. However, the data shown in Figure 8 were averaged over the interface area and do not consider the local behavior at the interface, which for short weld times was more uneven owing to the progressive breakup of the manganese coating (Figure 7(a)). With longer welding times (>1 seconds), when the coating became dispersed, the IMC layer became more uniform across the joint line, but its average thickness was still lower than that seen in the uncoated welds (Figure 7(c)).

## IV. DISCUSSION

In ultrasonic metal welding, deformation largely occurs by shear parallel to the plane of the sheet weld members and is concentrated within a thin surface layer of less than 100  $\mu\text{m}$  at the weld line.<sup>[12,15,16]</sup> The linear displacement at the interface is generally relatively small (5 to 10  $\mu\text{m}$ ), but because of the high frequency (20 kHz), the strain rate and accumulated strain are very high, even though the welding time is short.<sup>[15,18,25]</sup> The accepted mechanism for weld formation involves the development and progressive spreading of micro-welds.<sup>[15–18]</sup> This occurs by breakdown of the oxide on the sheet surfaces by abrasion at contacting perturbations, under the applied pressure and shear that occur across the joint line, due to the high frequency linear translation of the weld members, leading to the rapid development of a sticking condition at the weld interface. The sheets surface condition can thus be expected to affect the contact mechanics, and rate of microbond evolution and heat generation, in the early stages of welding.<sup>[16,17]</sup> As the welding time increases, the number of microwelds and the net welded area rapidly expand, leading to the majority of the heat being generated by plastic work<sup>[15,16,18]</sup>, and the weld strength consequently increases. In similar metal welds, this eventually leads to failure during mechanical testing by nugget pullout.<sup>[14,15]</sup> In this case, the subsequent decrease in weld strength seen for longer welding times is related to the increasing penetration of the sonotrode tips into the sheet surfaces, which causes thinning of the weld area.<sup>[14,15]</sup> However, with dissimilar welds produced between aluminum and magnesium, failure normally occurs at the joint interface due to the rapid growth of a brittle IMC layer, which dominates the fracture behavior.<sup>[19]</sup>

The growth behavior of the IMC layer in USWs between uncoated aluminum and magnesium sheets has previously been described in detail,<sup>[19]</sup> under identical conditions to those used in the current study. In this work, the intermetallic reaction layer was found to initially form in isolated islands at the weld interface, which are associated with the development of micro-welds where, as the temperature rises, interdiffusion first becomes significant. The  $\text{Al}_{12}\text{Mg}_{17}$  phase was found to form first on the aluminum side of the weld interface because it contains the highest proportion of magnesium, which is the fastest diffusing species in either of the two matrices.<sup>[32–34]</sup> The  $\text{Al}_{12}\text{Mg}_{17}$  IMC islands then rapidly spread and coalesced to form a continuous layer within a welding time of only 0.25 seconds. When the intermetallic layer is non-continuous, diffusion can occur more quickly along the interface between the IMC and the matrix, facilitating island growth.<sup>[32]</sup> However, once the layer becomes continuous, diffusion has to take place through the intermetallic layer, which acts as a barrier. After the  $\text{Al}_{12}\text{Mg}_{17}$  phase formed a continuous layer, a second IMC layer comprising the  $\text{Al}_3\text{Mg}_2$  phase was seen to develop on the aluminum side of the interface, which grew more quickly and became the thickest component of the reaction layer at longer weld times. At excessive welding times (>1 second), melting was observed at the interface between the IMC

reaction layer and the magnesium sheet, through the  $(\text{Mg})_{\text{SS}} + \text{Mg}_{17}\text{Al}_{12} \rightarrow \text{L}$  eutectic reaction present in the Al-Mg system,<sup>[19,21]</sup> which limited the layer thickness and caused it to start to reduce in the baseline data shown in Figure 8 for welding times greater than ~1 second.

Kinetic modeling using the parabolic growth law fitted to static experimental data has been previously used to show that the growth rate of the continuous IMC reaction layer is more than double that expected under static conditions.<sup>[19]</sup> This difference has been mainly attributed to USW increasing the growth rate due to the deformation taking place during welding causing microcracking in the brittle reaction layer as it develops, which allows short-circuit diffusion through the layer. However, the generation of large excess vacancy concentrations at the weld interface by the high strain rate ( $10^3$ <sup>[18,25]</sup>) dynamic deformation induced by the USW process is also thought to influence the early nucleation stages of the reaction when the layer is still discontinuous.<sup>[18,19,32]</sup>

### A. Cold Spray Coating

The aluminum cold spray coating was applied to the magnesium sheet in an attempt to separate the site of deformation and heat generation, which is concentrated at the join line in USW,<sup>[12,16,31]</sup> from the bimetallic Al-Mg interface. In principle, this should have two main advantages: (i) the IMC reaction rate is extremely sensitive to temperature<sup>[19,20,32]</sup> and (ii) the factors discussed above, that lead to an acceleration of the reaction kinetics under dynamic conditions, would be mitigated as they are largely localized to a narrow deformation layer on either side of the contacting sheet surfaces.

Although the cold spray coating did not lead to a significant increase in peak failure strength in the lap shear tests, it has been shown to improve the overall mechanical performance of the joints, particularly at longer welding times (Figures 3 and 4). In the pre-coated samples, the lap shear strengths exhibited a plateau in maximum strength with welding time, but more importantly their failure energy increased by 30 pct for optimum welding times (0.4 seconds) and became more than double than that of the uncoated welds for longer welding times (Figure 3(b)). However, failure still occurred predominantly at the interface between the magnesium alloy and the cold spray coating, leading to the coating being peeled off the sheet surface (Figures 5(a) and (b)). This occurred not only because this was the new location where the IMC reaction layer developed during welding, albeit at a lower rate, but also because bonding of the cold spray coating with the substrate does not achieve 100 pct efficiency, as it is attached by a combination of cold welding and mechanical locking.<sup>[30]</sup> Nevertheless, the improved fracture energy of the cold spray-treated welds can be attributed to the large reduction in growth rate of the IMC reaction layer that this coating provided.

Although the cold spray coating produced a rougher surface than on the uncoated magnesium sheet, which could potentially affect the dissipation of energy at the

weld line during USW, the temperatures recorded at the center of the weld interface were very similar between the welds produced with uncoated and coated samples. Unfortunately, the temperature differential between the immediate surface, where the heat is predominantly generated in USW, and at the depth of the coating interface with the magnesium substrate (100  $\mu\text{m}$ ) is difficult to determine. Modeling results by Elangovan *et al.*<sup>[31]</sup> suggest that at such a short distance from the weld line, the temperature difference would be expected to be quite small and of the order of 10 to 20 K, owing to the high conductivity of aluminum. It is therefore interesting to see if the reduced thickness of the IMC layer in the coated weld samples can be attributed solely to the temperature differential, or if kinetic factors related to the lower level of deformation below the weld contact surfaces play a significant role. From the parabolic growth law, the one-dimensional diffusion-controlled growth rate of IMC layer thickening can be expressed as

$$\frac{dx}{dt} = \frac{k}{x} \quad [1]$$

where  $x$  is the layer thickness and  $k$  is the conventional rate constant, given by

$$k = k_0 e^{\left(-\frac{Q}{RT}\right)} \quad [2]$$

( $R$  is Boltzmann's constant and  $T$  is absolute temperature). Reliable values for the kinetic constants,  $k_0$ , and,  $Q$ , the activation energy, have been previously determined from static annealing experiments in this system<sup>[19,20]</sup> and are reproduced in Table 1. Using these data, the thermal histories that gave the peak temperature measurements shown in Figure 2 have been used to predict the expected reaction layer thickness, by integration across the measured thermal cycles in discrete time steps. The results of this analysis are depicted in Figure 9 where predictions are given in as a function of welding time. This exercise was also repeated with the thermal cycles scaled to reflect (i) a progressive reduction in the peak temperature below the sheet surface and (ii) an under-read error of up to 10 pct in the maximum thermocouple measurements. The predicted curves are also compared to the actual average reaction layer thicknesses measured in the welds made with pre-coated and uncoated magnesium sheet. As has been discussed previously,<sup>[19]</sup> it can be seen that the curves calculated using rate constants determined from static conditions under-predict the growth rate in the welds made with uncoated magnesium sheet by a factor of at least a half, even if it is assumed that the thermocouple temperature measurements under-read by 10 pct.

In contrast, the points for the measured IMC layer thickness in the pre-coated magnesium welds lie very close to the predicted values for the line reflecting peak

**Table 1. Kinetic Growth Rate Constants for the IMC Reaction in the Al-Mg System Taken from Ref. [19]**

$k_0$ ( $\mu\text{m}^2 \text{s}^{-1}$ )	$Q$ ( $\text{kJ mol}^{-1}$ )
$5 \times 10^4$	65

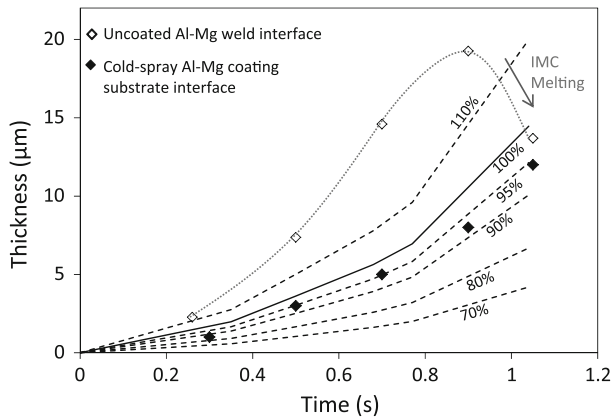


Fig. 9—Reaction layer thickness predictions from thermal cycles measured at the Al-Mg joint interfaces in welds with no coating, using static growth rate constants (solid line) and showing (i) the effect of a 10 pct increase, due to a thermocouple under-reading and (ii) a range of possible reductions in peak temperature below the joint line at the interface between the Al cold spray coating and Mg substrate (dashed lines). The predictions are compared to the actual IMC layer thicknesses measured for welds produced with uncoated and cold spray-coated Mg sheet (symbols).

temperatures of the order of 95 pct of that measured at the weld interface. For a weld time of 0.8 seconds' duration, this would correspond to a reduction in temperature of ~20 K, which is close to that expected for the temperature differential between the weld interface and the depth below the sheet surface at the base of the coating.<sup>[31]</sup> By comparison with the results for the uncoated weld, it can therefore be concluded that the much lower IMC reaction rate found when using aluminum cold spray-coated magnesium sheets is in line with expectation, based on the temperature at the displaced bimetallic interface, under conditions where there is little influence of the welding process other than to provide a heat source in the joint area. In terms of reducing the reaction rate, the cold spray coating has thus performed as well as could be expected, in that by displacing the reaction, a small depth from the weld interface, it has prevented the accelerated reaction kinetics normally seen when the welds are produced between uncoated sheets, where the growth rate is enhanced by the high level of deformation experienced close to the weld interface.<sup>[18,19]</sup>

### B. Mn Barrier Coating

The Mn-PVD coating was selected as a barrier coating in an attempt to inhibit the formation of Al-Mg IMCs that normally embrittle welds between aluminum and magnesium.<sup>[4-9]</sup> The PVD method was able to produce a thin continuous coating on the magnesium sheet, but the mechanical properties of the welds were only marginally improved relative to those produced with uncoated materials. Figure 3(b) showed that the lap shear strengths were almost identical, with no extended plateau region at peak strength as seen for the cold spray-coated samples. However, the joint fracture energies were again superior to those of welds produced with an uncoated magnesium sheet, but the difference reduced more with longer welding times than for the cold spray pre-coated samples.

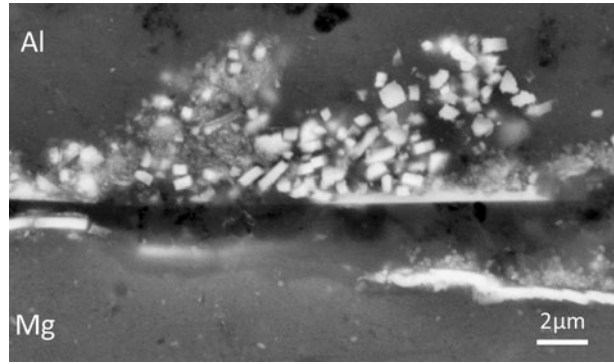


Fig. 10—Extreme example of the breakup of the manganese coating seen at the edge of the weld area with a welding time of 0.3 s.

Despite the higher surface hardness of the manganese-coated magnesium sheet, the peak temperatures recorded during welding were nearly identical to those seen in the uncoated control welds (Figure 2), except at very short welding times, and eutectic melting between magnesium and the IMC layer ( $\text{Mg}_{SS} + \text{Mg}_{17}\text{Al}_{12} \rightarrow \text{L}^{[19]}$ ) initiated at a similar welding time. Differences in interface temperature between the uncoated and coated samples as a function of weld time can, therefore, not be responsible for the reduction in average IMC layer thickness observed in the welds produced when the manganese-coated magnesium sheet was used.

Although the microstructures of pure manganese PVD coatings have themselves not been reported, work on similar coatings suggests they would be expected to be nanocrystalline in nature<sup>[35,36]</sup> and have a high hardness and low ductility. Because in USW the sheet surface is initially subjected to abrasion under sliding conditions and following adhesion high levels of local deformation occur at the interface, it was expected that a brittle barrier coating would struggle to survive intact for prolonged welding times. However, the results in Figure 7 show that the manganese coating started to breakup quite early in the welding process. An extreme example of this behavior is shown in Figure 10 from the edge of the weld area where folding had occurred at the interface and the manganese coating had fractured into small particles, of the order of 0.5 µm in length. Within the weld center, the coating did not breakup as quickly (Figure 7) and still seems to have reduced the average reaction rate by protecting significant areas of the magnesium surface, at least for short weld times (<0.5 seconds). With more prolonged weld durations, the coating became fully dispersed within the deformation zone near the weld interface, but overall the average IMC layer thickness still remained lower than that seen in welds where a barrier layer was not used (Figure 8). The blocking of interdiffusion between magnesium and aluminum where the coating did survive thus still had a noticeable effect on the mean growth rate of the IMC layer. The more irregular, and on average thinner, reaction layer that developed in the welds produced with Mn-coated sheets thus resulted in more difficult crack propagation at the weld interface and the more modest improvement in the fracture energy noted above.



## V. CONCLUSIONS

Two methods have been investigated for improving the poor joint performance typically found in Al-Mg dissimilar welds, which, in this system, results from the rapid growth of a thick IMC reaction layer, namely; (i) separation of the join line from the weld interface by the use of a thick (100  $\mu\text{m}$ ) aluminum cold spray coating and (ii) the introduction of a thin (1  $\mu\text{m}$ ) manganese PVD diffusion barrier layer, both applied to the magnesium sheet surface prior to welding.

A large improvement was noted for the fracture energy of the dissimilar joints in lap shear tests conducted on high power USWs with the cold spray-coated magnesium sheet and a smaller improvement was found with the Mn barrier coating. In each case, the peak temperatures measured at the weld interface were very similar to that seen with uncoated materials and differences in the IMC growth rate could, therefore, be attributed to the direct effect of the coatings. Both coatings were found to reduce the average thickness of the IMC layer, but not to a level where fracture at the weld interface could be fully avoided.

Of the two coatings, the thick cold spray coating had a greater effect on reducing the rate of intermetallic reaction in the Al-Mg couple, because it displaced the bimetallic interface from the weld line to the interface between the coating and the magnesium substrate. Kinetic modeling has been used to show that this benefit can be attributed to the reaction kinetics reverting to the rate expected under static conditions. This reduced the IMC growth rate by 50 to 70 pct because at the weld line the high strain rate dynamic deformation in USW normally enhances diffusion at the interface and through the IMC layer. In comparison, the thin PVD barrier coating was found to rapidly break up early in USW and become dispersed throughout the deformation layer with increasing welding time, which reduced its effectiveness. Nevertheless, the manganese coating still decreased the average IMC layer growth rate as it was able to prevent interdiffusion across a significant proportion of the interface area at short welding times.

## ACKNOWLEDGMENTS

This work was funded by the EPSRC through LATEST2, Light Alloys Towards Environmentally Sustainable Transport (EP/G022402/1). The authors are grateful to Professor X. Zhang of the Beijing Institute of Aeronautical Materials and Dr S. Ganguly of the Welding Engineering and Laser Processing Centre, Cranfield University, for producing the cold spray and Mn-PVD coatings, respectively, and T. Burman of Novelis U.K. and Dr T. Wilks of Magnesium Elektron for the provision of materials.

## OPEN ACCESS

This article is distributed under the terms of the Creative Commons Attribution License which permits any

use, distribution, and reproduction in any medium, provided the original author(s) and the source are credited.

## REFERENCES

1. D. Carle and G. Blount: *Mater. Des.*, 1999, vol. 20, pp. 267–72.
2. A. Jambor and M. Beyer: *Mater. Des.*, 1997, vol. 18, pp. 203–09.
3. X. Cui, S. Wangand, and S.J. Hu: *Mater. Des.*, 2008, vol. 29, pp. 381–87.
4. R. Borrisutthekul, Y. Miyashita, and Y. Mutoh: *Sci. Technol. Adv. Mater.*, 2005, vol. 6, pp. 199–204.
5. P. Venkateswaran, Z.-H. Xu, X. Liand, and A.P. Reynolds: *J. Mater. Sci. Eng.*, 2009, vol. 44, pp. 4140–47.
6. V. Firouzdor and S. Kou: *Metall. Mater. Trans. A*, 2010, vol. 41A, pp. 2914–35.
7. D.-H. Choi, B.-W. Ahn, C.-Y. Lee, Y.-M. Yeon, K. Song, and S.-B. Jung: *Intermetallics*, 2011, vol. 19, pp. 125–30.
8. J. Yan, Z. Xu, Z. Li, L. Li, and S. Yang: *Scripta Mater.*, 2005, vol. 53, pp. 585–89.
9. A. Gerlich, P. Su, and T.H. North: *Sci. Technol. Weld. Join.*, 2005, vol. 10, pp. 647–52.
10. T.A. Barnes and I.R. Pashby: *J. Mater. Process. Technol.*, 2000, vol. 99 (1–3), pp. 62–71.
11. T.A. Barnes and I.R. Pashby: *J. Mater. Process. Technol.*, 2000, vol. 99 (1–3), pp. 72–79.
12. H.C.P. Daniels: *Ultrasonics*, 1965, vol. 3, pp. 190–96.
13. Y. Gao and C. Doumanidis: *ASME J. Manuf. Sci. Eng.*, 2002, vol. 124 (2), pp. 426–34.
14. R. Jahn, R. Cooper, and D. Wilkosz: *Metall. Mater. Trans. A*, 2007, vol. 38A, pp. 570–83.
15. D. Bakavos and P.B. Prangnell: *Mater. Sci. Eng. A*, 2010, vol. 527, pp. 6320–34.
16. J.L. Harthoorn: Doctoral Thesis, De Technische Hogeschool Eindhoven, 1978.
17. Y.-R. Jeng and J.-H. Horng: *ASME J. Tribol.*, 2001, vol. 123, pp. 725–31.
18. Y.-C. Chen, D. Bakavos, and P.B. Prangnell: *Acta Mater.*, 2012, vol. 60, pp. 2816–28.
19. A. Panteli, J.D. Robson, I. Brough, and P.B. Prangnell: *Mater. Sci. Eng. A*, 2012, vol. 556, pp. 31–42.
20. E.M. Tanguet Njiokep, M. Salamon, and H. Mehrer: *Defect Diffus. Forum*, 2001, vols. 194–199, pp. 1581–86.
21. V. Rothova and J. Cermak: *Proc 15th Int. Metallurgical & Material Conference*, Czech Republic, Metal, 2006, pp. 1–8.
22. J.L. Murray: *Binary Alloy Phase Diagrams*, 2<sup>nd</sup> ed., T.B. Massalski, ed., ASM International, Metals Park, OH, vol. 1, 1990, pp. 169–71.
23. Y.S. Sato, S.H.C. Park, M. Michiuchi, and H. Kokawa: *Scripta Mater.*, 2004, vol. 50, pp. 1233–36.
24. D. Dietrich, D. Nickel, M. Krause, T. Lampke, M.P. Coleman, and V. Randle: *J. Mater. Sci.*, 2011, vol. 46, pp. 357–64.
25. I.E. Gundaz, T. Ando, E. Shattuck, P.Y. Wong, and C.C. Doumanidis: *Scripta Mater.*, 2005, vol. 52, pp. 939–43.
26. R.W. Richards, R.D. Jones, P.D. Clements, and H. Clarke: *Int. Mater. Rev.*, 1994, vol. 39, pp. 191–209.
27. L.M. Zhao and Z.D. Zhang: *Scripta Mater.*, 2008, vol. 58, pp. 283–86.
28. L. Liu, X. Liu, and S. Liu: *Scripta Mater.*, 2006, vol. 55, pp. 383–86.
29. M. Asgar-Khan and M. Medraj: *Proc. Materials Science and Technology (MS&T)*, October 5–9, 2008, Pittsburgh, PA, pp. 1029–41.
30. W.B. Choi, L. Li, V. Luzin, R. Neiser, T. Gnäupel-Herold, H.J. Prask, S. Sampath, and A. Gouldstone: *Acta Mater.*, 2007, vol. 55, pp. 857–66.
31. S. Elangovan, S. Semeer, and K. Prakasan: *J. Mater. Process. Technol.*, 2009, vol. 209, pp. 1143–50.
32. J.D. Robson, A. Panteli, N. Iqbal, and P.B. Prangnell: *Sci. Technol. Weld. Join.*, 2012, vol. 17, pp. 447–53.
33. J. Philibert: *Mater. Sci. Forum*, 1994, vols. 155–156, pp. 15–30.
34. S. Fujikawa and K. Hirano: *Mater. Sci. Eng. A*, 1977, vol. 27A, pp. 25–33.
35. W. Lauwerens, A. De Boeckb, M. Thijs, S. Claessens, M. Van Stappen, and P. Steenackers: *Surf. Coat. Technol.*, 2001, vols. 146–147, pp. 27–32.
36. M. Reffass, C. Berziou, C. Rébère, A. Billard, and J. Creus: *Corros. Sci.*, 2010, vol. 52, pp. 3615–23.